Adaptive Calibration of the Tandem-L Ground Demonstrator

Jan Paul Kroll*, **Marwan Younis***, **Gerhard Krieger***, **Tobias Rommel***

*Microwaves and Radar Institute
German Aerospace Center (DLR)
Germany
email: jan.kroll@dlr.de

Abstract: *We propose an adaptive calibration scheme for multi-channel Synthetic Aperture Radar (SAR) that allows for an uninterrupted SAR operation while performing the calibration. The parameters of the planned Tandem-L ground demonstrator are applied to a simulation tool to estimate the errors and residual errors using said calibration scheme.*

1. Introduction

Imbalances between the channels in a multi-channel SAR system lead to a degradation of the antenna pattern. This results in a deterioration of the Signal-to-Noise Ratio (SNR) and resolution. To mitigate these errors, the properties and variations of the channels have to be determined and the channels have to be adapted, based on this knowledge. This is done by calibrating the system [1]. In elevation digital beam-forming techniques such as SCan-On-REceive (SCORE) are employed to surmount the limitations of a conventional Synthetic Aperture Radar (SAR). To realize SCORE a narrow receive beam is formed and steered in real time to the direction of arrival of the SAR echo signal [2]. Due to the real-time beam-forming operation, the calibration of the elevation channels has to be performed on-board. The internal calibration for active phased arrays can be executed by employing a calibration signal that is coupled in close to the antenna and evaluated at the Digital Beam-forming Unit (DBU), [3, 4]. It allows to calibrate the system and simultaneously perform the transmit or receive operation. The measurement error for the proposed calibration method is mitigated by estimating the drift via a least square linear polynomial fit. In order to compensate the drift, the variable elements are set using the estimated values. The time of the calibration (measurement and correction) is adapted based on the drift variation of the elements.

A mathematical model to describe the effects in a multi-channel SAR system is developed. The model includes the system, the signals and the error sources. On Radio Frequency (RF) level the error sources are: drifts, gain compression [5, 6], mutual coupling between the antenna elements, coupling between the signal paths and errors due to the Analog-to-Digital Converters (ADCs). To estimate the errors and residual errors after calibration a simulation tool based on the developed mathematical models is created.

Tandem-L is a proposal for a highly innovative SAR mission to observe dynamic processes globally [7]. In order to demonstrate the SAR modes, algorithms, data processing and the calibration the Tandem-L ground demonstrator (TD-L BoDem) is being built. Our model is applied to the TD-L BoDem system and implemented in the simulation tool.

978-3-944976-30-3 ©2021 DGON

2. Tandem-L Ground Demonstrator

Fig. 1 shows the TD-L BoDem system for the receive operation. The transmit signals can be recorded as well, but here we focus on receive. It is a system with $N = 32$ channels. The coupling of the calibration signal (CalTone) is after the antenna input in the Amplification Unit (AU). It can be switched between the even $(0, 2, \dots)$ and the uneven $(1, 3, \dots)$ numbered channels. The path of the echo signal is marked in red, the CalTone in green. The signal is down-converted in the Radio Frequency Unit (RFU). At DBU level the channels are weighted according to the digital beam-forming and the CalTone is evaluated. After the DBU the elevation channels are combined.

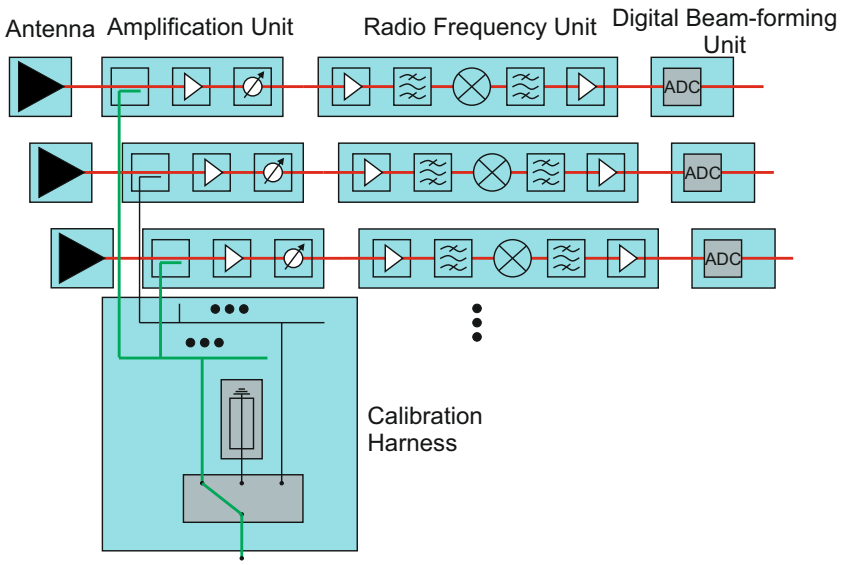

Figure 1: Tandem-L ground demonstrator system design. The receive case is displayed. The path of the echo signal is marked in red and the path of the calibration signal in green.

3. Signal Models

A SAR system transmits a series of pulses. Each pulse is a frequency modulated signal. We modeled the echo signal as a signal from an extended target. This can be implemented by adding the fields of the randomly distributed point scatterers inside the target. In base-band representation and frequency domain the multiply scattered field can be described by:

$$S_{\mathrm{RX}}(f) = A \cdot \mathrm{rect}\left(\frac{f - f_{\mathrm{c}}}{B}\right) \cdot e^{-j\frac{\pi\tau}{B}(f-f_{\mathrm{c}})^2} \cdot \sum_{k=1}^{K} B_{\mathrm{k}} e^{-j2\pi\Delta t_{\mathrm{k}}(f+f_{\mathrm{c}})} C_{\mathrm{2way}}(\theta_{\mathrm{k}}, \varphi_{\mathrm{k}}, \theta_0, \varphi_0), \quad (1)$$

with amplitude A, the rectangular function rect(), frequency f, carrier frequency f_{c}, bandwidth B, pulse duration τ and amplitude and phase of the kth scatterer B_{k}, with K being the number of scatterers. The scatterer influence B_{k} is modeled by complex, zero-mean Gaussian random variables. Δt_{k} represents the round-trip time of scatterer k. C_{2way} stands for the two-dimensional two-way antenna pattern for the scatterer located at θ_{k} and φ_{k}, while the pattern maximum is steered to θ_0 and φ_0. The echo signal is then normalized to the nominal input power.

The CalTone is modeled in the frequency domain as:

$$S_{\mathrm{CT}}(f) = A_{\mathrm{CT}} \cdot \mathrm{sinc}\left\{\tau_{\mathrm{CT}}(f - f_{\mathrm{CT}})\right\}, \tag{2}$$

where the CalTone has an amplitude of A_{CT}, a duration of τ_{CT} and a frequency of f_{CT}. The sinc function is defined as: $\mathrm{sinc}(x) = \frac{\sin(\pi x)}{\pi x}$.

4. Error Models

To describe the effects in a multi-channel system mathematical models are developed in the following for each error source.
The temperature drift describes the change of the amplitude and phase over temperature respectively time. It is modeled as a complex polynomial function, where the variable of the polynomial is the temperature. The temperature of the components varies with slow time t_{s}, where the temperature distribution is dependent on the instrument design. The temperature distribution is modeled via a two-dimensional discretized heat equation.
The coupling is modeled as a time-delayed, amplitude and phase weighted replica of the signal that is added to the original one.
If the amplifier input power is increased above a certain point, the amplification decreases and the linear relation ceases to exist. The non-linear effect can be described using the Volterra series [5, 6], which also takes the memory of the amplifier into account. The Volterra series transitions into a power series for a memory-less system. Because of the complexity and computational limitations we chose to model the gain compression via power series. The coefficients are calculated based on the input-output characteristics of the amplifier. Due to the zero-point symmetry of the amplitude amplification the even coefficients of the power series are approximately zero $a_{\mathrm{2n}} \approx 0$; for $n = 0, 1, \ldots$. The gain compression can therefore be modeled by:

$$G_{\mathrm{C}}(t) = \sum_{n=0}^{\infty} a_{\mathrm{2n+1}} \cdot \left(S_{\mathrm{in}}(t)\right)^{2n+1}, \tag{3}$$

where S_{in} is the input signal to the amplifier. The power series is terminated after the sixth term ($n = 3$).
Two models for noise are implemented: additive noise and phase noise. The absorption noise of passive or active components, characterized by their noise figure, is modeled by applying the former. The latter, phase noise, is applied to model down-converters.
To model the AUs' behavior various models have to be employed. Apart from the temperature drift, coupling, gain compression and noise, there is also the variable gain and phase and the frequency transfer function.
The modeled effects of the ADCs are: First, an aliasing of the spectrum due to the sampling of the signal. Second, sample and timing jitter leading to synchronization errors. Third, the quantization of the signal and the resulting errors.

5. Internal Calibration Concept

The purpose of the internal calibration is to measure the instrument drift over time and to correct it. For our model we divided the instrument RF and digital chain into several layers, indicated in Fig. 1, where each layer can be considered individually. The influences of the individual layers are described by their respective Transfer Function (TF), e.g. H_{RFU}. The calibration is performed simultaneously to the SAR operation.

5.1. Drift Evaluation

In the suggested internal calibration system, the CalTone, after generation, passes the CalTone harness before it is coupled to the SAR echo signal at the AU, depicted for the receive operation in Fig. 1 in green. The evaluation is done in the DBU by analyzing the amplitude and phase of the measured signal with respect to the initial values. This allows a measurement of the TF and drift in the components passed by the CalTone. The evaluation is done at the frequency of the CalTone. The drift can be expressed as the difference between the initial value of the TF and the actual one.
In Fig. 2 an example of the signal spectrum at DBU level is depicted. The frequency of the CalTone can be varied to account for frequency dependencies of the TFs. It can also be located within the spectrum of the frequency modulated signal.

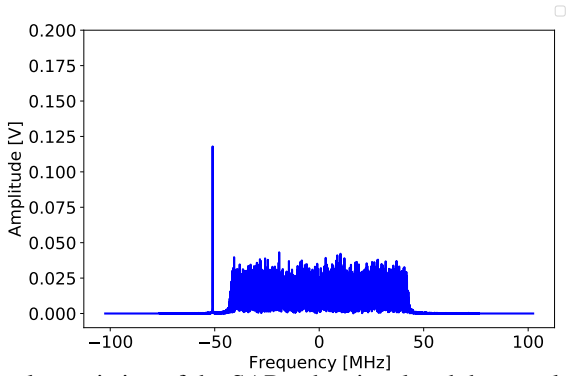

Figure 2: Spectrum at DBU level, consisting of the SAR echo signal and the coupled CalTone at frequency $f_{\mathrm{CT}} = -51\ MHz$.

5.2. Measurement Errors

The measured TF at the CalTone frequency f_{CT} can be expressed as:

$$H_{\mathrm{RX}}(t_{\mathrm{s}}) = \frac{[H_{\mathrm{A}}(t_{\mathrm{s}})S_{\mathrm{RX}}(t_{\mathrm{s}}) + H_{\mathrm{CTH}}(t_{\mathrm{s}})S_{\mathrm{CT}}]}{|S_{\mathrm{CT}}|^2} \cdot S^*_{\mathrm{CT}} H_{\mathrm{AU}}(t_{\mathrm{s}}) H_{\mathrm{R}}(t_{\mathrm{s}}) + N. \tag{4}$$

The TFs of the receiver (RFU and DBU) were summarized as H_{R} and H_{AU} is the TF of the AU. H_{A} summarizes the TFs for the echo signal previous to the AU, i.e., the radiators and antenna harnesses. H_{CTH} stands for the CalTone harness TF and N for the noise. We can rearrange the equation to get the desired TFs (green) and a multiplicative and an additive error term (red):

$$H_{\mathrm{RX}}(t_{\mathrm{s}}) = H_{\mathrm{AU}}(t_{\mathrm{s}})H_{\mathrm{R}}(t_{\mathrm{s}}) \cdot H_{\mathrm{CTH}}(t_{\mathrm{s}}) + \frac{H_{\mathrm{AU}}(t_{\mathrm{s}})H_{\mathrm{R}}(t_{\mathrm{s}})H_{\mathrm{A}}(t_{\mathrm{s}})S_{\mathrm{RX}}(t_{\mathrm{s}})}{S_{\mathrm{CT}}} + N. \tag{5}$$

5.3. Drift Estimation

For an echo signal of a multiply scattered field the error related to the echo signal as well as the error from the noise is distributed around zero. To improve the measurement, we make a least square linear polynomial fit of a number of previously measured values. The error due to the coupling is an offset that cannot be mitigated by the proposed estimation method. However, the nominal coupling coefficient is known and can be used to correct the measurement.

6. Simulation Results

The mathematical models are implemented in a simulation tool. The parameters for the TD-L BoDem are applied to the simulation tool, given in Table 1.

Table 1: Instrument parameter for the simulation.

Parameter	Value
B	$85\,\mathrm{MHz}$
τ	$80\,\mu\mathrm{s}$
A	$0.5\,\mathrm{mV}$
A_{CT}	$1.28\,\mathrm{V}$
f_{CT}	$-25.5\,\mathrm{MHz}$
τ_{CT}	$80\,\mu\mathrm{s}$

The performance is determined with the Standard Deviation (SD) of the error.
The results of the estimation are shown in Fig. 3. The amplitude is shown in the upper and the phase in the lower plot. The actual values are the blue and green lines, the measured the red and orange dots. The estimated values are depicted by the black lines. The amplitude error SD improves through the estimation from $SD_{\mathrm{A,m}} = 0.11\,\mathrm{dB}$, for the measured values, to $SD_{\mathrm{A,e}} = 0.04\,\mathrm{dB}$ and the phase error SD from $SD_{\mathrm{P,m}} = 6.8°$ to $SD_{\mathrm{P,e}} = 2.6°$.

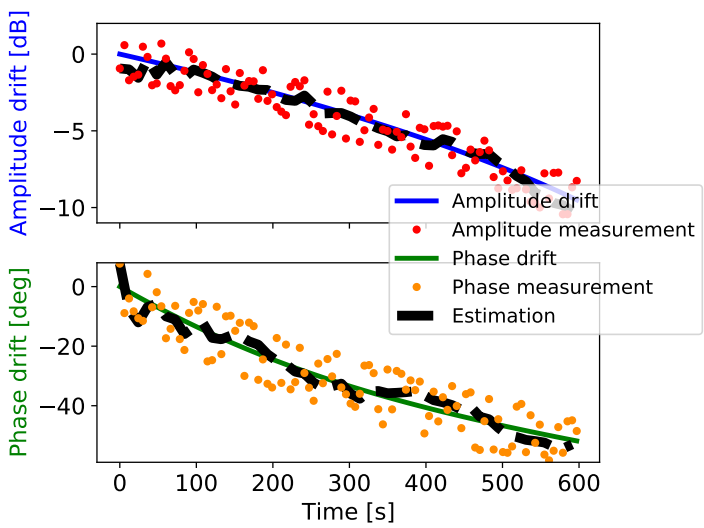

Figure 3: The upper plot shows the amplitude and the lower the phase for the actual (blue and green), measured (red and orange) and estimated (black) drift.

The drift while adaptively calibrating the system is shown in Fig. 4.

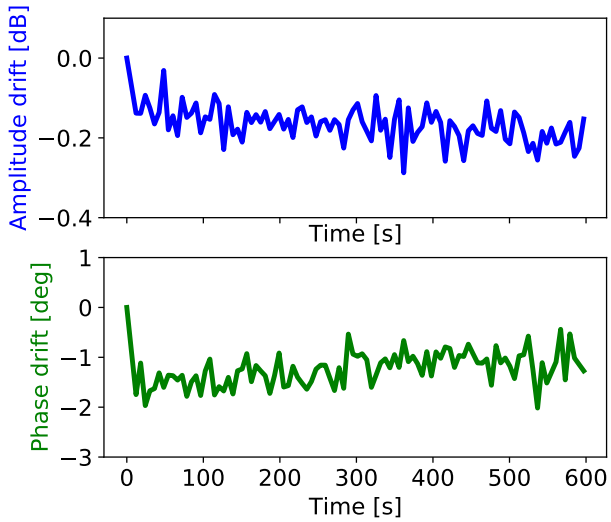

Figure 4: The upper plot shows the amplitude and the lower the phase of the instrument drift while adaptively calibrating.

7. Conclusion

Based on the parameters for the Tandem-L ground demonstrator an adaptive calibration method is introduced. With this method it is possible to keep the drift at a nearly constant level with only small variations. The performance is shown with results from a simulation tool.

References

[1] A. Freeman, "SAR calibration: an overview," *IEEE Transactions on Geoscience and Remote Sensing*, vol. 30, no. 6, pp. 1107–1121, 1992-11.

[2] M. Suess, B. Grafmueller, and R. Zahn, "A novel high resolution, wide swath SAR system," in *IGARSS 2001. Scanning the Present and Resolving the Future. Proceedings. IEEE 2001 International Geoscience and Remote Sensing Symposium (Cat. No.01CH37217)*, vol. 3. IEEE, 2001.

[3] B. Brautigam, M. Schwerdt, and M. Bachmann, "An efficient method for performance monitoring of active phased array antennas," *IEEE Transactions on Geoscience and Remote Sensing*, vol. 47, no. 4, pp. 1236–1243, 2009-04.

[4] J. P. Hoffman, S. Horst, L. Veilleux, H. Ghaemi, and S. Shaffer, "Digital calibration system enabling real-time on-orbit beamforming," in *2014 IEEE Aerospace Conference*. IEEE, 2014-03, pp. 1–11.

[5] M. Schetzen, *The Volterra and Wiener theories of nonlinear systems*. Wiley, 1980.

[6] Y. Wan, T. J. Dodd, and R. F. Harrison, "MODELING OF POWER AMPLIFIER NONLINEARITIES USING VOLTERRA SERIES," *IFAC Proceedings Volumes*, vol. 38, no. 1, pp. 785–790, 2005.

[7] A. Moreira, G. Krieger, M. Younis *et al.*, "Tandem-l: A highly innovative bistatic SAR mission for global observation of dynamic processes on the earth's surface," *IEEE Geoscience and Remote Sensing Magazine*, vol. 3, no. 2, pp. 8–23, 2015-06.